

## Function of a minus-end-directed kinesin-like motor protein in mammalian cells

Jurgita Matuliene<sup>1</sup>, Russell Essner<sup>1</sup>, Jung-Hwa Ryu<sup>1</sup>, Yukihiisa Hamaguchi<sup>2</sup>, Peter W. Baas<sup>3</sup>, Tokuko Haraguchi<sup>4</sup>, Yasushi Hiraoka<sup>4</sup> and Ryoko Kuriyama<sup>1</sup>

<sup>1</sup>Department of Genetics, Cell Biology, and Development, University of Minnesota, Minneapolis, MN55455, USA

<sup>2</sup>Biological Laboratory, Tokyo Institute of Technology, Tokyo, Japan

<sup>3</sup>Department of Anatomy, University of Wisconsin Medical School, Madison, WI 53706, USA

<sup>4</sup>Kansai Advanced Research Center, Communications Research Laboratory, Kobe, Japan

\*Author for correspondence (e-mail: ryoko@lenti.med.umn.edu)

Accepted 6 September; published on WWW 3 November 1999

### SUMMARY

**CHO2 is a mammalian minus-end-directed kinesin-like motor protein present in interphase centrosomes/nuclei and mitotic spindle fibers/poles. Expression of HA- or GFP-tagged subfragments in transfected CHO cells revealed the presence of the nuclear localization site at the N-terminal tail. This domain becomes associated with spindle fibers during mitosis, indicating that the tail is capable of interaction with microtubules in vivo. While the central stalk diffusely distributes in the entire cytoplasm of cells, the motor domain co-localizes with microtubules throughout the cell cycle, which is eliminated by mutation of the ATP-binding consensus motif from GKT to AAA. Overexpression of the full-length CHO2 causes mitotic arrest and spindle abnormality. The effect of protein expression was first seen around the polar region where microtubule tended to be bundled together. A higher level of protein expression induces more elongated spindles which eventually become disorganized by losing the**

**structural integrity between microtubule bundles. Live cell observation demonstrated that GFP-labeled microtubule bundles underwent continuous changes in their relative position to one another through repeated attachment and detachment at one end; this results in the formation of irregular number of microtubule focal points in mitotic arrested cells. Thus the primary action of CHO2 appears to cross-link microtubules and move toward the minus-end direction to maintain association of the microtubule end at the pole. In contrast to the full-length of CHO2, overexpression of neither truncated nor mutant polypeptides resulted in significant effects on mitosis and mitotic spindles, suggesting that the function of CHO2 in mammalian cells may be redundant with other motor molecules during cell division.**

Key words: Microtubule, Mitotic spindle, Minus-end motor, CHO cell

### INTRODUCTION

One of the most fundamental processes in cells is that of cell division, wherein two daughter cells are produced from a single cell. During cell division, cells assemble the mitotic/meiotic spindle that is responsible for equal segregation of the genetic material into progenies. The spindle is associated with a number of motor molecules that exert forces necessary to form and maintain the normal size of bipolar spindles (Barton and Goldstein, 1966, for a review). A series of mitotic events, such as pole separation during prophase, chromosome congression to the metaphase plate, and chromosome movement/spindle elongation in anaphase cells are believed to be triggered by the change in balance between the forces. In order to understand the mechanism of mitosis and its regulation, it is therefore important to identify and characterize individual forces acting at the different parts of the spindle at different mitotic stages.

Over ninety motor molecules have so far been identified and

are further subdivided into distinctive subclasses (Hirokawa, 1998, for a review). One such subclass designated as the Kar3 subfamily includes a total of twenty-five or so members; they are unique in a sense that they contain the mechanochemical motor domain at the C terminus and move toward the minus-end of microtubules, the opposite direction to that of conventional as well as the majority of other kinesin-like motor molecules (Walker et al., 1990; McDonald et al., 1990; Endow et al., 1994; Kuriyama et al., 1995). Members of this subclass are thus believed to be an antagonist of plus-end-directed motors belonging to the BimC subfamily. All of C-terminal motor proteins have a short oligopeptide stretch at the neck between the central stalk and the motor domain, which has recently been demonstrated to be essential for determination of the directionality of proteins' movement toward the minus-end direction (Sablin et al., 1998; Endow and Waligora, 1998).

Functional analysis of the minus-end-directed motors in dividing cells has been initiated by genetic analysis of yeast

*KAR3* (Meluh and Rose, 1990) and *Drosophila ncd* (McDonald and Goldstein, 1990; Endow et al., 1990). *KAR3* in *Saccharomyces cerevisiae* is essential for karyogamy, which is believed to be mediated by the ability of the Kar3p protein to bundle microtubules and pull two connecting nuclei into a close proximity (Meluh and Rose, 1990). Although the motor protein is essential for meiosis (Bascom-Slack and Dawson, 1997), its function in mitotic cells is redundant with other motor activities, thus the loss of the protein's function causes only partial mitotic arrest and delay in cell growth (Meluh and Rose, 1990). In addition, the ability of Kar3p to promote microtubule depolymerization at the minus-end was shown to be important for maintenance of the proper shape of the spindle structure (Saunders et al., 1997).

Mutation in *Drosophila ncd* causes a high rate of chromosome non-disjunction and chromosome loss in oocytes during meiosis (Davis, 1969). Frequent loss of mitotic chromosomes is also detected in early embryos. The absence of *ncd* motor activity results in the formation of diffuse and wide spindles with disorganized pole structures (Kimble and Church, 1983). Based on detailed microscopic observation of fly oocytes, it has been suggested that the major role of this minus-end-directed motor is to assemble and stabilize spindle poles in the absence of typical microtubule-nucleating centers at the pole (Matthies et al., 1996). Despite extensive studies on Kar3p and *ncd*, the lack of molecular information of other minus-end-directed motors in different species prevents generalization of functional properties of minus-end-directed motors in the mechanism of spindle function and its regulation. This is particularly prominent in cultured mammalian cells in which a wealth of morphological, cytological and physiological information is available for the study of mitosis.

Using monoclonal anti-mitotic spindle antibodies as a probe, we identified a first minus-end-directed motor protein in mammalian cells (Kuriyama et al., 1995). The protein termed CHO2 was originally identified as a centrosomal antigen which was later shown to be present in interphase nuclei and spindle fibers/poles as well (Sellitto et al., 1992; Ohta et al., 1995). In order to evaluate the function of the mammalian minus-end-directed motor protein, we expressed CHO2 polypeptides in CHO cells by transient transfection. Here we report mitotic inhibition caused by overexpression of the functional, full-coding sequence of CHO2, but not truncated/mutant proteins. The degree of spindle abnormality is parallel to the level of protein expression, and the detailed microscopic observation suggested the importance of both motor and microtubule binding/bundling activities of CHO2 for formation and maintenance of functional bipolar spindles.

## MATERIALS AND METHODS

### Preparation of CHO2 deletion/mutation constructs

#### Deletion constructs

The cDNA fragments encoding different regions of CHO2 (accession number X83576) were subcloned into the multicloning site of the eukaryotic expression vector, pCMV-HA. The plasmid was engineered to include the start codon and the in-frame nine amino acid sequence of hemagglutinin (HA) epitope upstream of the multicloning

site. This allowed transfected cells to express proteins tagged with HA sequence at the N terminus. The following six constructs were prepared according to the standard cloning procedures (Fig. 1A): pCMV-HA-CHO2F (CHO2 full-coding sequence, amino acids 1-622), pCMV-HA-CHO2SM (CHO2-17a: the region corresponding to the stalk at amino acids 110-257 and motor domain at amino acids 258-622; Kuriyama et al., 1995), pCMV-HA-CHO2M (motor domain, amino acids 258-622), pCMV-HA-CHO2S (stalk domain, amino acids 110-257), pCMV-HA-CHO2TS (tail-stalk domain, amino acids 1-257), pCMV-HA-CHO2T (tail domain, amino acids, 1-89). CHO2F (*Bam*HI/*Kpn*I fragment), CHO2ST (*Bam*HI/*Afl*II fragment), CHO2T (*Bam*HI/*Mse*I-265 fragment) were isolated from the pVL1392-CHO2 construct (Kuriyama et al., 1995), whereas CHO2SM (*Eco*RI/*Xho*I fragment), CHO2M (*Afl*II/*Xho*I fragment) and CHO2S (*Eco*RI/*Afl*II fragment) were derived from pGEX-CHO2-17a (Kuriyama et al., 1995).

To express CHO2 proteins fused with green fluorescent protein (GFP), cDNA inserts (CHO2F, CHO2SM, CHO2ST) were first isolated from pCMV-HA constructs using flanking restriction sites in the multicloning site of the vector, then subcloned into pEGFP-C1 (Clontech, La Jolla, CA).

### Constructs with site-specific mutation

A CHO2 mutant carrying the altered sequence in the ATP-binding motif from GKT to AAA (amino acid positions 365 to 367) was created using the ExSite PCR-Based Site-Directed Mutagenesis Kit (Promega, Madison, WI) according to the manufacturer's protocol as reported previously (Sharp et al., 1997b). Mutants of CHO2 full-length (CHO2F'), stalk-motor (CHO2SM') and motor (CHO2M') were constructed by replacing the *Afl*II/*Hind*III fragment in pCMV-HA plasmids carrying the wild-type sequence with the mutated *Afl*II/*Hind*III fragment derived from pVL-CHO2Δ1' (Sharp et al., 1997b). The change in the nucleotide sequence was confirmed by sequence analysis.

### Cell culture and protein expression

CHO cells were grown as monolayers in Ham's F-10 medium containing 10% fetal calf serum (FCS: HyClone, Logan, UT) with antibiotics and 15 mM Hepes at pH 7.2 (Kuriyama et al., 1995). For preparation of M phase cells, cells on coverslips were first treated with 2.5-5 mM thymidine for 12-16 hours to arrest the cell cycle at S and G<sub>1</sub>/S stages. After washing out the thymidine, cells were cultured in the F-10 medium for an additional 5 hours, then exposed to 0.05 μg/ml nocodazole for 4-5 hours. The drug was removed gently from the cells which were further cultured in a fresh medium for 20-50 minutes at 37°C before fixation.

Transfection of CHO cells was performed by employing three different protocols: microinjection, electroporation and lipofection (Kofron et al., 1998). All procedures provided essentially identical results. For microinjection, plasmid DNA 100-500 μg/ml was prepared in the injection buffer (100 mM KCl, 10 mM KPO<sub>4</sub> at pH 7.4) and introduced directly into cells using a Narishige micromanipulator. For electroporation, trypsinized cells were placed in a cuvette at 3-8×10<sup>6</sup> cells/ml, then mixed with plasmid DNA at a final concentration of 50 μg/ml. A pulse of 700 μF at 300 V was applied to cells by an Electro Cell Manipulator 600 (BTX, San Diego, CA). Liposome/lipid-mediated DNA transfection was performed using 0.6-2 μg/ml plasmid DNA mixed with either Lipofectamine (Life Technologies, Gaithersburg, MD), SuperFect (Qiagen, Chatsworth, CA), or FuGene (Boehringer-Mannheim, Indianapolis, IN) transfection reagents according to the manufacturer's protocol. After 12 to 24 hours induction, cells were washed with PBS and fixed with cold methanol.

### Immunofluorescence staining and fluorescence quantitation

Proteins induced in transfected cells were analyzed by immunoblots

and immunofluorescence staining as previously described (Kuriyama et al., 1995). For immunostaining, methanol-fixed cells were rehydrated with 0.05% Tween-20-containing phosphate buffered saline (PBS-Tw20) and treated with a mixture of primary antibodies which contained either (a) monoclonal mouse (Berkeley Antibody Co., Richmond, CA) or rat (Boehringer-Mannheim) anti-HA and affinity purified polyclonal rabbit anti-CHO2 antibodies, (b) monoclonal anti-chicken  $\beta$ -tubulin (Amersham, Arlington Height, IL) and polyclonal CHO2 antibodies, or (c) monoclonal anti-tubulin and polyclonal anti-HA (Santa Cruz Biotechnology, Santa Cruz, CA) antibodies. After incubation at 37°C for 30 minutes, cells on coverslips were washed with PBS-Tw20 and treated with secondary antibodies (fluorescein-conjugated anti-mouse or anti-rat plus Texas red-conjugated anti-rabbit antibodies). Microscopic observation was made on an Olympus BH-2 microscope with epifluorescence optics.

The level of CHO2 expression was quantitated by digital analysis of immunofluorescence intensity of transfected mitotic cells using the MetaMorpho software package (Universal Image Co., version 2.0) as described before (Ohta et al., 1995).

### Live cell observation

#### Phase-contrast video microscopy

CHO cells grown on photoetched coverslips (Bellco Glass Co., Vineland, NJ) were transfected with the clone encoding GFP-tagged CHO2F, CHO2SM and CHO2TS, and further incubated at 37°C overnight in a CO<sub>2</sub> incubator. Before starting video recording, the medium was changed to the FCS-containing F-10 medium without NaHCO<sub>3</sub>. The coverslip-containing dishes were wrapped with parafilm and placed on the microscopic stage which was maintained at 37°C by a stage temperature controller (Fryer Company Inc., Edina, MN) and an air curtain incubator (Nicholson Precision Instruments Inc., Bethesda, MD). After identification of cells expressing GFP-tagged CHO2 proteins by fluorescence microscopy, time-lapse images of the cells were recorded using a Dage-Mti video camera (model 65) (Michigan City, IN).

#### Fluorescence microscopy

For live observation of fluorescently-stained mammalian cells, the computer-controlled microscope system DeltaVision (Applied Precision Inc., Seattle, WA) was assembled in a temperature-control room as described previously (Hiraoka and Haraguchi, 1996; Haraguchi et al., 1997). The microscope system is based on an Olympus inverted microscope IX70, equipped with a Peltier-cooled CCD PXL1400 (Photometrics, Ltd., Tucson, AZ), and controlled by a Silicon Graphics workstation Indigo2.

CHO or HeLa cells on a glass-bottom culture dish (MatTek Corp., Ashland, MA) were transfected by microinjection of the GFP-CHO2F fusion plasmid into nuclei. After culturing overnight in the presence of 80  $\mu$ g/ml kanamycin sulphate, cells were stained with 100 ng/ml Hoechst 33342 for 5-30 minutes, followed by washing three times with the fresh culture medium. Before microscopic observation, cells were incubated in a bovine serum (Gibco BRL) in a CO<sub>2</sub> incubator for at least 30 minutes, then 20 mM Hepes buffer (pH 7.4) was added to the medium. This allowed us to culture cells without CO<sub>2</sub> gas. Fluorescently labeled living cells were observed at 37°C using an Olympus oil immersion objective lens with a high numerical aperture

(UApo40/NA1.35). Time-lapse images were recorded at 1 minute intervals with an exposure time of 0.1-0.5 seconds.

## RESULTS

### Intracellular localization of CHO2 subdomains: identification of nuclear-localization and microtubule-binding sites

#### Protein localization in interphase cells

To analyze subregions of the CHO2 motor protein, we created a series of deletion constructs (Fig. 1A) and expressed HA-epitope-tagged truncated CHO2 polypeptides in CHO cells by transient transfection. Expression of recombinant proteins was confirmed by immunoblot analysis in whole cell lysates (Fig. 1B). Fig. 2 summarizes the subcellular distribution of individual polypeptides determined by fluorescence microscopy. We showed before that endogenous CHO2 is present in the nucleus in a cell cycle-dependent manner (Ohta et al., 1995). The site responsible for nuclear localization is present in the tail, since expression of the tail-containing sequence, including the full-length (Full) (Fig. 2A-A'', B-B''), tail-stalk (TS) (Fig. 2F-F'') and tail (T) (Fig. 2G-G''), resulted in positive immunostaining of the nucleus with both HA and CHO2 antibodies. In some cells transfected with the CHO2F sequence, a part of the expressed protein was detected in the cytoplasm as well (arrows in 2A', A''). Double immunostaining with CHO2 and tubulin antibodies revealed the exogenous protein associated with the microtubule network in the cytoplasm of interphase cells (arrows in 2B' and B''). Motor and stalk domains lack the nuclear localization site, therefore, HA-tagged CHO2SM, CHO2M and CHO2S accumulated in the cytoplasm. While the motor-containing sequences bound to cytoplasmic microtubules (Fig. 2C-C'', D-D''), the stalk alone spread in entire cytoplasm (Fig. 2E-E''). These results indicate that CHO2 is capable of interaction with microtubules through the C-terminal motor domain. It is noteworthy that microtubules in the cell with overinduced CHO2F (A-A'', B-

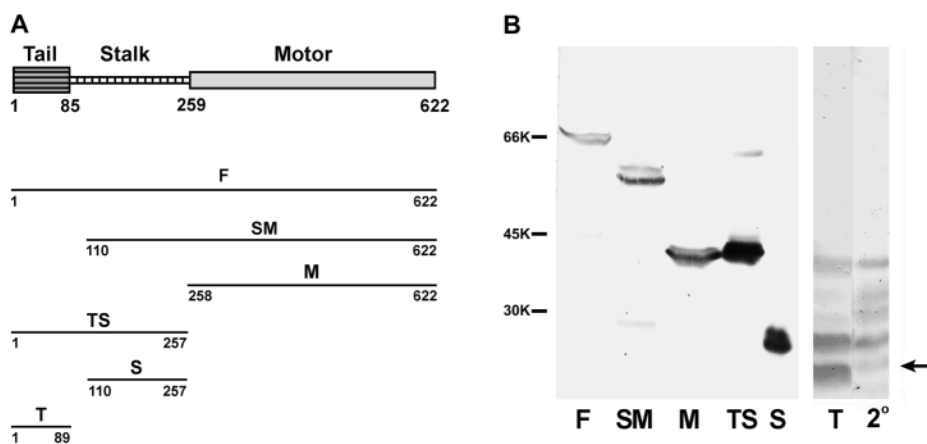


**Fig. 1.** (A) A map of deletion constructs of CHO2 expressed in CHO cells by transient transfection. The number underneath at the end of each clone represent amino acid numbers encoded by the clones. (B) Immunoblot analysis of CHO2 polypeptides expressed in CHO cells by transient transfection. Proteins prepared from transfected whole cells were run on 10% gels and transferred into nitrocellulose membranes which were further incubated with monoclonal anti-HA rat antibody. A nitrocellulose strip in Lane 2° was incubated with the alkaline phosphatase conjugated secondary antibody alone. An arrow indicates the position of CHO2T.

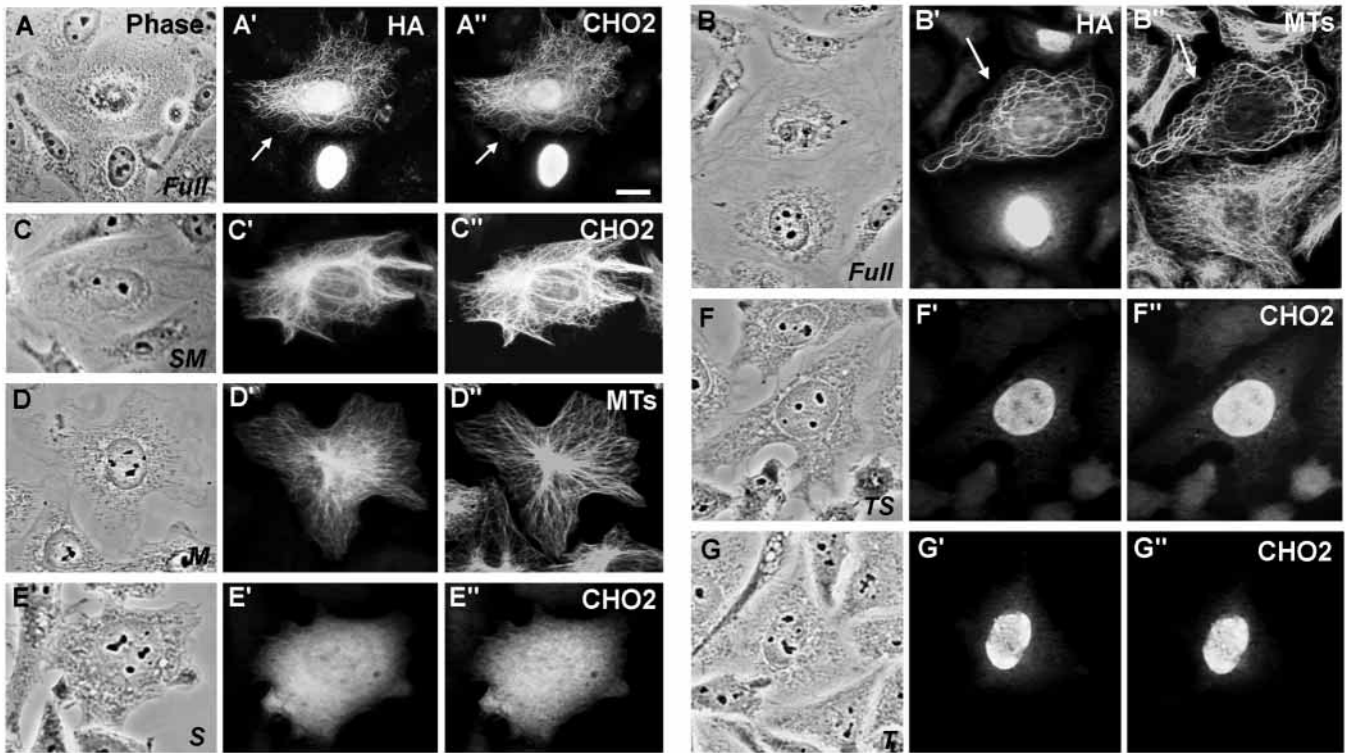


**Fig. 2.** Immunolocalization of expressed full and truncated CHO2 in transfected CHO interphase cells. The same cells are seen by phase-contrast (A-G) and fluorescence microscopy after double staining with monoclonal (A', C', E'-G') or polyclonal (B', D') HA, and polyclonal CHO2 (A'', C'', E'-G'') or monoclonal tubulin (B'', D'') antibodies. Shown are cells that express CHO2F (A-B), CHO2SM (C), CHO2M (D), CHO2S (E), CHO2TS (F), and CHO2T (G). The tail contains the nuclear localization site, thus CHO2TS and CHO2T are found in the nucleus. In addition to the nucleus, CHO2F is sometimes seen in the cytoplasm in association with the microtubule network (arrows in A'-A'' and B'-B''). While CHO2SM and CHO2M are present along cytoplasmic microtubules, CHO2S is diffusely distributed in the entire cytoplasm. Bar, 10 µm.

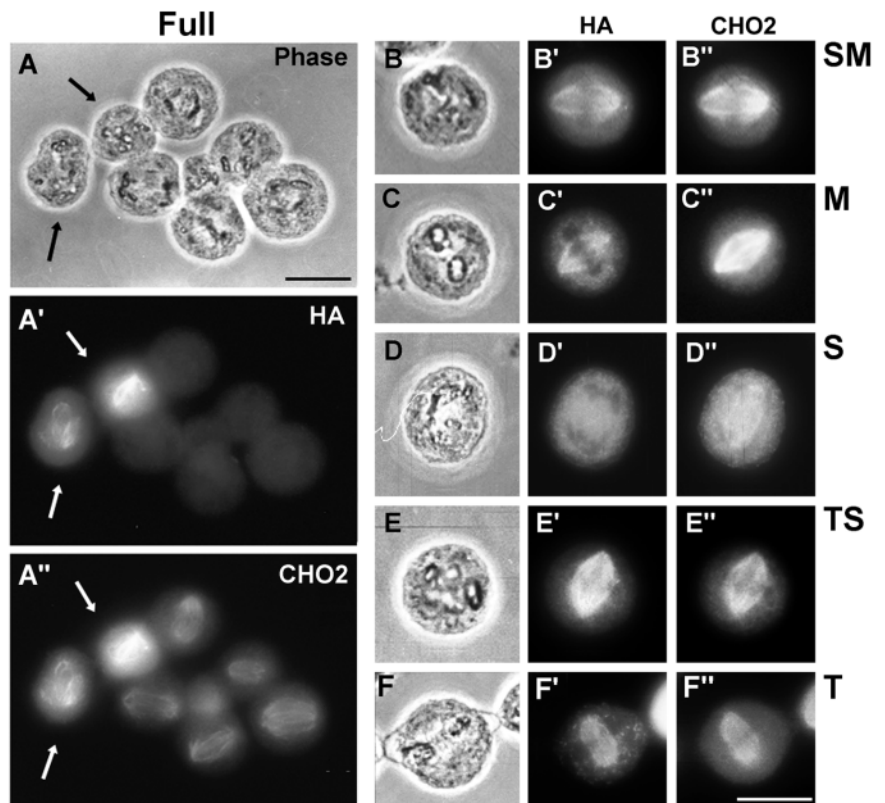


**Fig. 3.** Immunolocalization of exogenous full-length and truncated CHO2 in transfected CHO cells in mitosis. The same cells are seen by phase-contrast (A-F) and fluorescence microscopy after double staining with monoclonal HA (A'-F') and polyclonal CHO2 (A''-F'') antibodies. Cells express CHO2F (A), CHO2SM (B), CHO2M (C), CHO2S (D), CHO2TS (E), and CHO2T (F). All proteins, except CHO2S, co-localize at the mitotic spindles. Arrows in A-A'' indicate two transfected cells containing abnormal mitotic spindles. Bars, 10 µm.

B'') or CHO2SM (C-C'') were often cross-linked, while no such microtubule bundles were detected in cells overexpressing the motor domain alone (D-D'').

#### Protein localization in mitotic cells

The epitope-tagged CHO2 polypeptides were further examined in mitotic cells. Fig. 3A-A'' includes synchronized M phase cells double immunostained with HA (3A') and CHO2 (3A'') antibodies. Indicated by arrows are two transfected cells expressing exogenous CHO2F probed by both the antibodies. Like endogenous CHO2, HA-tagged molecules became localized at spindle fibers, though the shape of the mitotic spindles is considerably distinct from that of control spindles (see below). CHO2SM and CHO2M also displayed the affinity to spindle microtubules (3B,C). In contrast, the domain corresponding to the stalk alone appears to be insufficient for localization at the spindle, leading to an accumulation of the high level of fluorescent background in the transfected cell cytoplasm (3D'). CHO2T and CHO2TS contain the nuclear localization site in their sequence. During M phase, however, the proteins are in the cytoplasm and present along the length of spindle microtubules as shown in 3E-E'' and 3F-F''. These results indicate that the CHO2 tail possesses an intrinsic capability to interact with microtubules *in vivo*.

#### Expression of mutant CHO2

To assess the role of motor activity of CHO2, we created mutant proteins in which three amino acids corresponding to the ATP-binding consensus motif were altered from GKT to AAA (amino acid positions, 365 to 367). The mutant CHO2 motor domain (CHO2M') was completely devoid of the capability of microtubule interaction in both interphase and mitotic cells (data not shown). This may imply that the CHO2 motor domain interacts with microtubules only through the ATP-binding sequence. When the mutant protein

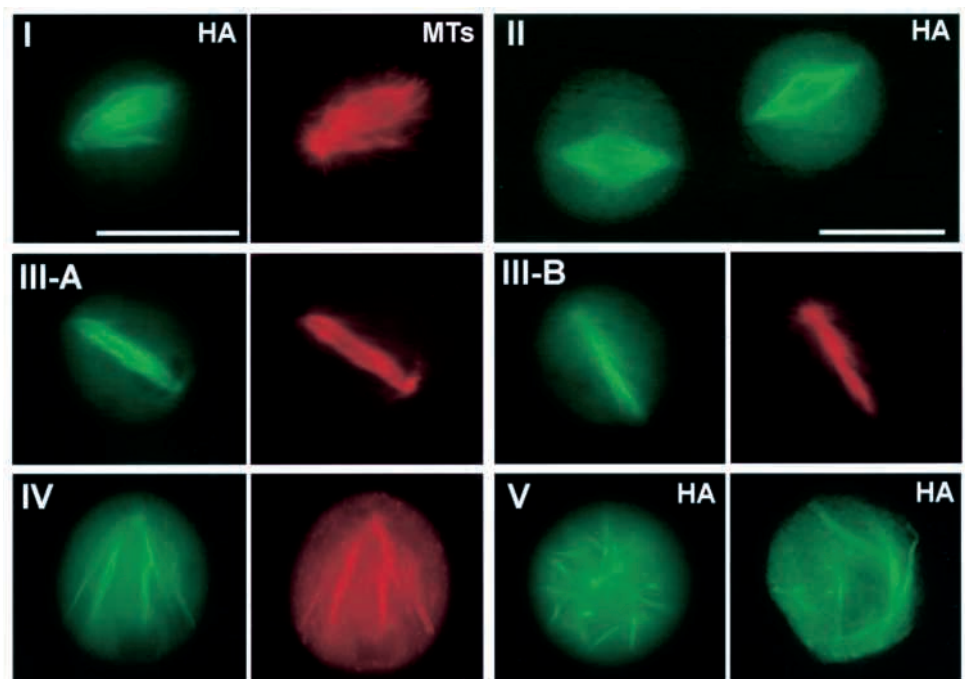
corresponding to the full-coding sequence of CHO2 (CHO2F') was expressed, it was detected in the exactly identical location (nuclei and spindle fibers) to the wild-type protein. Like CHO2F, it was also sometimes seen in the cytoplasm in association with microtubules which appeared to be cross-linked together and running around the nucleus (data not shown). Supposing microtubule bundling results from the presence of more than one microtubule-binding sites, CHO2F' must form a dimer complex or contain additional microtubule-interacting site(s) other than that included in the motor and tail domains.

#### Overexpression of the full-length CHO2 causes mitotic abnormality

##### Formation of abnormal mitotic spindles

In contrast to typical bipolar spindles formed in control cells, cells expressing the full length CHO2 often include the spindle in a wide range of morphological abnormalities (Fig. 3A-A''). Examination of over 500 transfected cells in mitosis has allowed us to classify such abnormal spindles into several categories (Fig. 4). Class I includes almost normal bipolar spindles with dislocated and/or splaying microtubules (Fig. 4-I). Spindle microtubules in Class II attach tightly at the polar region, thus tend to converge to the spindle pole in a steep angle. This results in the formation of a diamond shape spindle (II). In Class III, heavily bundled microtubules form thin and elongated spindles which are in either bipolar (III-A) or monopolar (III-B) arrangement. Chromosomes included in this type of spindles are generally scattered and poorly aligned at the metaphase plate (data not shown). Spindles in Class IV are composed of bundled microtubules which are connected at one end; the other microtubule end frays out widely to form a monopolar orientation (IV). In Class V, bundles of spindle microtubules totally lack any regular organization, running at different directions in a random manner (V).

**Fig. 4.** Classification of abnormal spindles into five categories. Mitotic cells expressing CHO2F were double immunostained with polyclonal HA (green) and monoclonal tubulin (red) antibodies. Class I: Bipolar spindles with dislocated and/or splaying out microtubules. Class II: Microtubules are tightly bundled around the pole, resulting in the formation of a diamond-shape of spindles. Class III: Thin and highly elongated spindles form either bipolar (III-A) or monopolar (III-B) organization. Class IV: Monopolar spindles composed of highly bundled microtubules. One end of microtubules splays out widely. Class V: Microtubule bundles do not form any regular organization. Bars, 10  $\mu$ m.



The degree of spindle abnormality correlates with the level of protein expression. Fig. 5 summarizes the intensity of HA immunofluorescence quantitated in cells containing abnormal spindles in different categories. While spindles in Class I and II are typically seen in cells with low abundance of exogenous CHO2F, cells expressing the moderate level of protein exhibit a broad range of spindle morphologies in all categories, predominantly in Class III. A higher level of protein expression results in the formation of heavier bundled and more randomly oriented microtubules. In fact, almost all cells expressing a high level of CHO2F include spindles categorized in Class V. These results suggest that the effect of protein expression becomes first apparent around the pole where the minus-end-directed motor protein is enriched (Kuriyama et al., 1995), and microtubules are cross-linked together more prominently than in any other locations. A higher level of protein expression induces thinner and more elongated spindles which are composed of highly bundled microtubule arrays along the entire length of the spindle. Microtubule-containing structures are eventually disorganized by loosing the integrity between bundles.

#### Mitotic inhibition

Conjugation of CHO2F with green fluorescent protein (GFP) allowed us to identify living cells expressing exogenous CHO2 proteins. Microscopic observations demonstrated that GFP-tagged molecules exhibited the exactly identical intracellular localization pattern to that of HA-CHO2F. In order to examine the effect of exogenous CHO2 on mitosis, we first monitored the cell cycle progression by recording transfected cells with a time-lapse video microscope. Fig. 6 includes a series of microscopic frames of nonsynchronized CHO cells taken at different time points. In this particular field, a total of twenty-eight non-transfected cells were identified to undergo normal mitosis and cytokinesis (1-28 in frames 1 to 12). They became round at the onset of M phase and completed cell division within 0.5-1.5 hours, which resulted in the production of two daughter cells of equal size. As confirmed by fluorescence microscopy (frame 12'), two cells (arrowheads) were expressing exogenous proteins. They were able to enter M phase, but became arrested at mitosis and remained round for about 6-8 hours. Despite their attempts to cleave, cell division was never completed. This inhibitory effect of CHO2F on cell division was further confirmed in an additional ten cells by time-lapse video microscopy. After entering the next cell cycle stage, one cell became binucleated (frame 12'). Indeed, nearly 20% of cells expressing CHO2F contained more than one nucleus ( $n > 700$ ), which is significantly more frequent than in control cells ( $< 2\%$ ).

#### Live cell observation by fluorescence microscopy

Using the fluorescence microscope system with precise temperature control (Hiraoka and Haraguchi, 1996; Haraguchi et al., 1997), we monitored the change in microtubule-containing structures in cells expressing GFP-tagged, full-length CHO2. Fig. 7A illustrates a live cell with the low level of exogenous CHO2F; it entered M phase and proceeded normal mitotic processes through prophase to telophase. At high levels of protein expression, cells became arrested at mitosis. As shown in Fig. 7B, the cell initiated to form highly bundled microtubule arrays which were attached at one end and

underwent continuous changes in their relative position to one another throughout the entire period of mitotic arrest. Through repeated attachment and detachment at one end, an irregular number of focal points becomes created in a random and temporal manner. Longer mitotic arrest tends to induce the less organized monoastral structure. It was also frequently noted that towards the end of mitotic arrest, microtubules were arranged to form a screw-like pattern as shown in frame 330'. The cell eventually exited from M phase; chromosomes decondensed and the spindle disassembled, but without completion of cell division (frame 990'). GFP fluorescence was recorded in six more CHO and HeLa cells which displayed a similar sequence described above. These results suggest that spindle microtubules associated with overexpressed CHO2F are cross-linked together and move around to change their relative position to one another through the motor activity of CHO2.

#### Overexpression of truncated/mutant polypeptides does not inhibit mitosis

In contrast to the full-coding sequence of CHO2, overexpression of neither truncated nor mutant polypeptides resulted in a significant increase in mitotic abnormalities (Fig. 3B-F). This could be due to the low amount of the truncated/mutant proteins produced in transfected cells. To establish the relationship between the level of protein expression and spindle abnormalities, we quantitated the fluorescence intensity of the HA epitope in cells expressing different CHO2 constructs. As summarized in Fig. 8, induction of CHO2 subfragments did not result in a substantial increase in the number of abnormal spindles at any level of protein expression. The mutant protein was, however, apparently more toxic than the truncated polypeptides, as nearly 50% of abnormal spindles were seen in cells with the highest level of

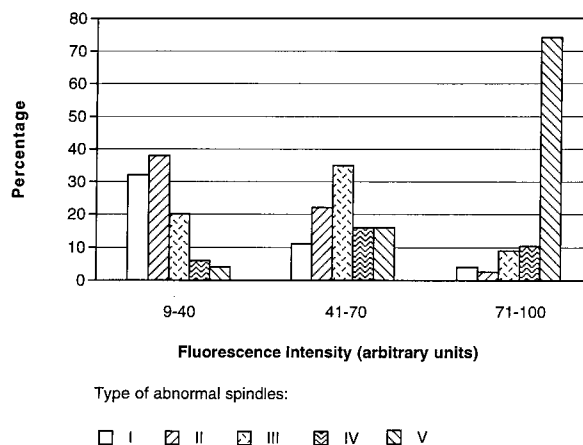


**Fig. 5.** The degree of spindle abnormality is correlated with the level of CHO2F expression in transfected cells. The amount of CHO2F was quantitated by MetaMorph as arbitrary units of HA immunofluorescence which were divided into three categories of low (9-40 units), medium (41-70 units) and high (71-100) expression. The histogram was constructed by combining the result of six separate experiments using both synchronized and non-synchronized cell populations. Spindles in Class I and II are common in cells expressing the low level of CHO2F. The higher the level of protein expression, the more severe the disorganized spindle in Class V.

CHO2F' expression. Virtually all abnormal spindles formed in cells expressing at any levels of truncated/mutant proteins were categorized in Class I. Time-lapse video microscopic analysis also showed that the cells could undergo normal mitosis and cell division. These results suggest that overexpression of only the fully functional CHO2F is capable of induction of abnormal spindles and mitotic inhibition. Thus, not only the motor but also microtubule binding/bundling activities are essential for the role of this minus-end-directed motor protein to assemble and maintain the functional bipolar spindle in mammalian cells.

## DISCUSSION

### Localization of CHO2 at the centrosome and nucleus

Like other conventional kinesins and kinesin-like proteins, mammalian CHO2 is composed of three subdomains: the C-terminal globular motor domain is connected with the N terminal tail through an  $\alpha$ -helical stalk. CHO2 was originally identified as an antigen localized at the centrosome (Sellitto et al., 1992). In contrast to endogenous CHO2, however, neither full nor truncated/mutant polypeptides were able to associate with the centrosome in transfected CHO cells (Figs 2 and 3). In order to target to the centrosome, exogenous proteins may have to be modified, or additional molecules may be required to recruit CHO2 to the centrosome.

In addition to the centrosome, CHO2 is localized at the interphase nucleus in a cell cycle-dependent manner (Ohta et al., 1995). The nuclear localization site(s) (NLS) was found to reside in the tail. A part of the NLS-containing CHO2 sequence also accumulates in the cytoplasm in association with the microtubule network. Since this was observed in cells expressing varying levels of exogenous proteins (J. Matuliene and R. Kuriyama, unpublished), the presence of the NLS-containing CHO2F in the cytoplasm might not be caused by the protein's overflow from the nucleus to the cytoplasmic compartment. Rather, translocation of the nuclear protein into the cytoplasm could represent a physiological event coupled with the cell cycle.

Although CHO2 is one out of twenty-five members of the Kar3 subfamily (Hirokawa, 1998), only a few, such as plk1 (Pidoux et al., 1996) and XCTK2 (Walczak et al., 1997), have so far been localized inside the nucleus. This is in contrast with Kar3p and ncd which are found in the cytoplasm. Therefore, nuclear localization may not represent a universal feature among minus-end-directed, C-terminal motor proteins. The amount of CHO2 in the nucleus changes

during the cell cycle progression (Ohta et al., 1995). CHO2 could be important for nuclear activities. Alternatively, the protein is synthesized and stored inside the nucleus until it is needed for mitosis during cell division. Excess CHO2 motor activities in the cytoplasm might cause changes in the cytoskeletal organization and/or distribution of cytoplasmic organelles in transfected cells. Keating et al. (1997) have reported that microtubules originating from the interphase centrosome are constitutively released from the centrosome

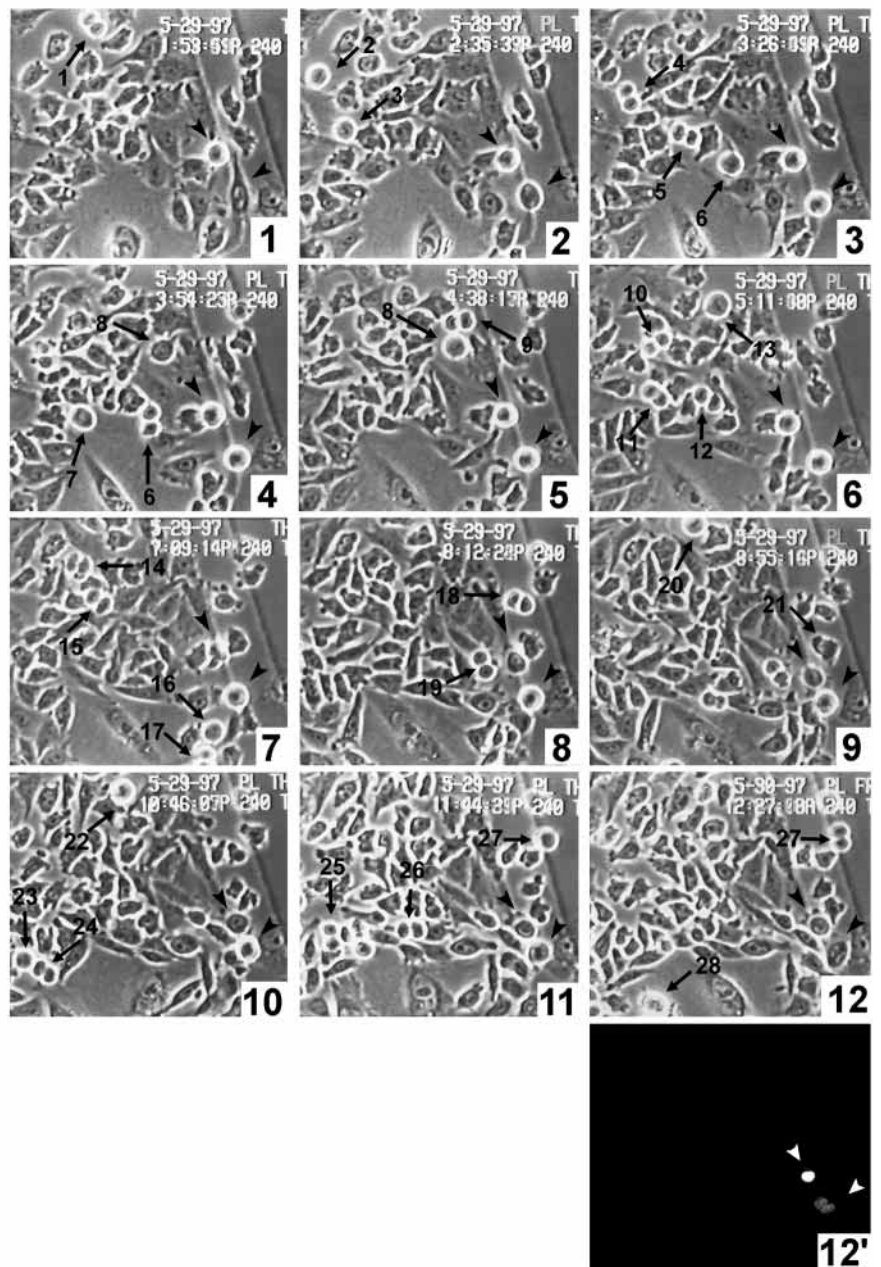


**Fig. 6.** Mitotic inhibition in cells overexpressing CHO2F. Cell cycle progression was monitored by time-lapse video phase-contrast microscopy. Frame #1-12 are images taken at different time points. Frame 12' corresponds to a fluorescence image of Frame 12, showing the presence of two transfected cells expressing GFP tagged CHO2F. While control cells, numbered 1-28, were able to complete normal cell division, two transfected cells (arrowheads) became arrested at M phase. After entering the next cell cycle generation, one cell became binucleated.

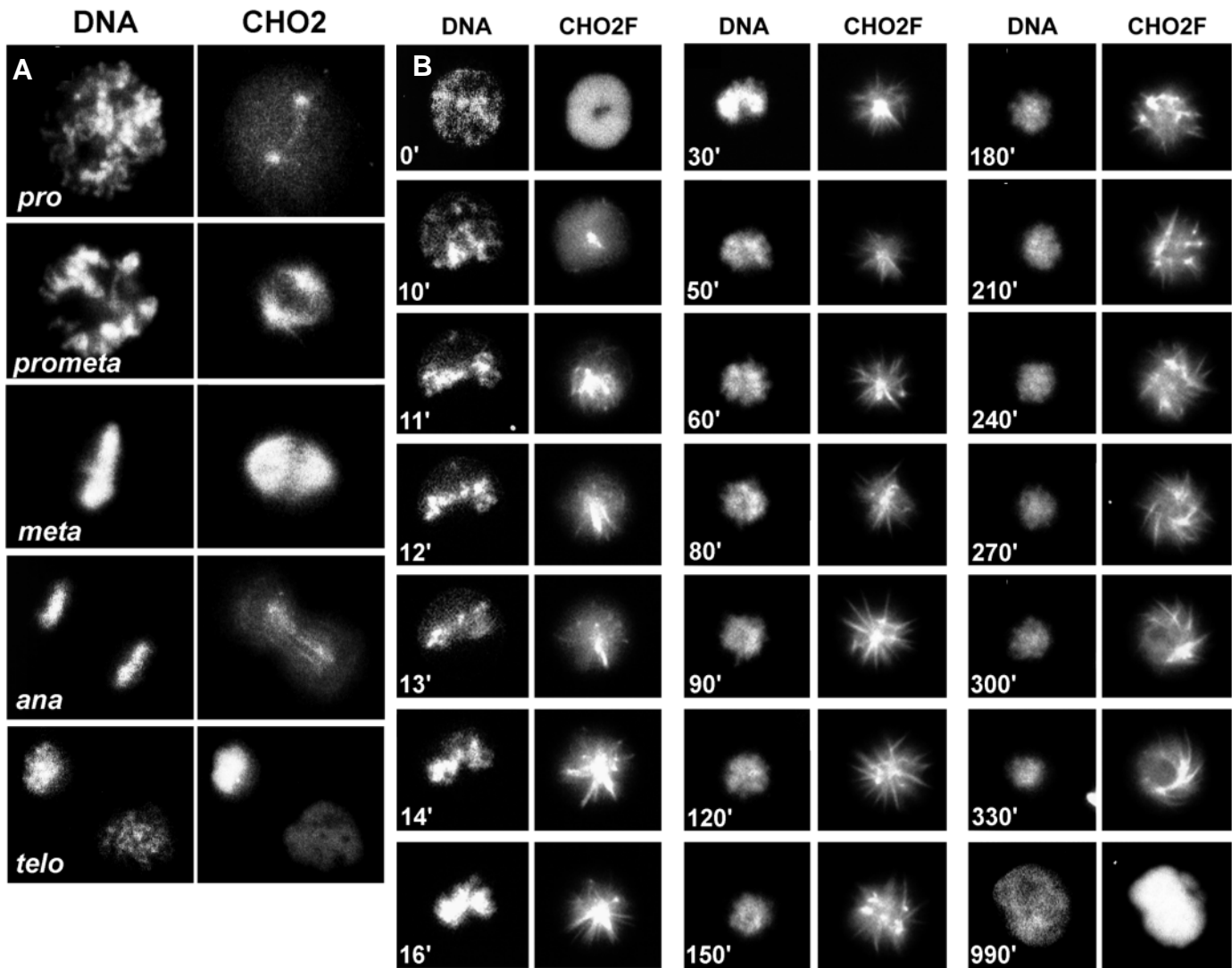


**Fig. 7.** Time-lapse images of a living mitotic cell expressing GFP-tagged CHO2F. Chromosomes were stained with Hoechst 33342, and the image of fluorescently labeled living cells were observed at 37°C on an Olympus inverted microscope IX70. (A) HeLa cell expressing the low level of CHO2F proceeds normal mitosis. (B) A CHO cells with the high level of CHO2F forms heavily bundled microtubules that undergo continuous changes in their relative position to one another throughout the mitotic arrest.

in cultured mammalian cells. Released microtubules are transported with their plus ends leading, which could be driven by a minus-end-directed motor. Since CHO2 is a minus-end-directed motor specifically localized at the centrosome (Sellitto et al., 1992), it would be interesting to examine whether the protein is involved in the process of detachment and/or transport of microtubules from the centrosome.

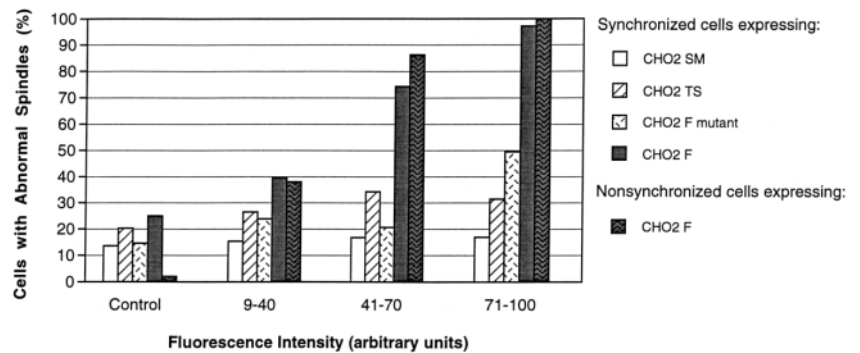
#### Microtubule-binding domains of CHO2

Comparison of the intracellular distribution of different subdomains allowed us to identify the presence of several microtubule-binding sites in CHO2. The mechanochemical motor domain interacts with microtubules through the ATP-binding consensus sequence in a nucleotide-dependent manner. By changing GKT to GKI or GKN in the consensus motif, Nakata et al. (1995) created the rigor-binding type mutation of the conventional kinesin heavy chain. When the GKT sequence

was replaced to AAA, we noted that the microtubule binding capacity of CHO2 motor domain was entirely lost. The C-terminal motor head of kinesin (Yang et al., 1989) and *ncd* (Moore et al., 1996) has been suggested to include another the ATP-independent microtubule-binding region around the SSRSH sequence, which represents one of the invariant motifs of all kinesin/kinesin-like proteins identified so far. Although this consensus sequence is included in CHO2 at amino acid positions 484 to 488, we were unable to detect any interaction of CHO2M' with microtubules in vivo. The apparent discrepancy may be derived from the difference in the microtubule-binding assay employed in each system (in vitro microtubule co-sedimentation vs protein association with microtubules in vivo), or, the ATP-independent microtubule-binding site of CHO2 may not be prominent in transfected cells.

Additional microtubule-binding activity is detected in the N-terminal globular tail, which appears to be common among

**Fig. 8.** Frequency histogram of abnormal spindles in CHO cells expressing different subregions and/or full-length mutant CHO2. The protein amount, quantitated by MetaMorph as arbitrary units of HA fluorescence, was divided into three categories as shown in Fig. 5. The experiment was repeated three more times to count total 150 spindle samples for each histogram. The synchronized cell population produced more abnormal spindles than non-synchronized cells. Almost all abnormal spindles formed in cells expressing at any levels of truncated/mutant polypeptides were categorized in Class I.



minus-end-directed motor proteins, such as *Drosophila ncd* (Chandra et al., 1993) and possibly yeast Kar3p (Meluh and Rose, 1990). However, a striking difference noted between CHO2 and *ncd* is their ability to cross-link microtubules together: while the *ncd* tail causes extensive microtubule bundling in vitro (Chandra et al., 1993; Karabay and Walker, 1999), the tail of CHO2 is able to bind to, but not bundle microtubules both in vitro (Kuriyama et al., 1995) and in vivo. Although two ATP-independent microtubule interaction sites have recently been identified in the *ncd* tail at amino acids 83-100 and 115-187 (Karabay and Walker, 1999), these sequences are poorly conserved in CHO2. It was also found that the size of the globular tail of *ncd* is over twice larger than that of the CHO2 tail. These differences may represent the functional diversity between mitotic and meiotic C-terminal motor proteins.

CHO2 cross-links microtubules in vivo and in vitro, which could be due to the presence of more than one microtubule-binding site in the protein. Supposing CHO2 forms a dimer complex as with the majority of other kinesin/kinesin-like proteins, it would be reasonable to speculate that overexpression of CHO2F (Fig. 2A-A'', B-B''), CHO2SM (Fig. 2C-C''), CHO2F', and possibly CHO2TS, induce microtubule bundling. In mitotic cells, however, none of the overexpressed proteins, except CHO2F, can display intense cross-linking activity of spindle microtubules. This may imply that either some microtubule-binding sites in CHO2 become inactivated during M phase, or additional microtubule-binding sites are required to connect spindle microtubules together during cell division.

### The function of CHO2

Compared with yeast Kar3p and *Drosophila ncd*, functional characterization of minus-end-directed motors has been limited in mammalian cells. CHO2 is the first-identified, mammalian motor protein of the Kar3 subfamily and we detected striking phenotypes in cells overexpressing the full-length protein. Microtubules become bundled to form highly elongated spindles; such bundled microtubules often converge to the pole with steep angle, resulting in the formation of a diamond shape of the spindle structure. Since cross-linking of spindle microtubules could facilitate microtubule sliding, it is likely that high levels of CHO2 motor activity make the spindle thin and long as it moves towards the minus-end of microtubules. In fact, *Drosophila* mutant cells lacking the *ncd* motor activity form short and barrel shaped spindles without focused poles (Kimble and Church, 1983). It is thus likely that the primary

function of CHO2 would be to maintain and stabilize the focus of the spindle microtubules at the pole. Since *ncd* (Matthies et al., 1996) and XCTK2 (Walczak et al., 1997) also display similar effects on spindle structures, members of the Kar3 subfamily appear to possess the common functional property in both mitotic and meiotic cells.

We are puzzled by the fact that overexpression of neither truncated nor mutant CHO2 polypeptides resulted in striking phenotypes in transfected M phase cells. In order to maintain the normal size of bipolar spindles, excess minus-end-directed CHO2 activities acting on the spindle fibers and poles have to be balanced with opposing forces generated by other motor proteins. Cells overexpressing truncated/mutant polypeptides fail to create molecules able to compete with the functional endogenous CHO2. In our preliminary experiments, it was observed that microinjection of monoclonal/polyclonal anti-CHO2 antibodies did not cause any inhibitory effects on mitosis (Y. Hamaguchi, J.-H. Ryu and R. Kuriyama, unpublished). We may have not employed appropriate procedures sensitive enough to detect subtle changes in the phenotype of microinjected cells. Alternatively, CHO2 could be functionally redundant with other motor proteins, which is important to protect cells from loss of essential motor activities. In fact, overlapping functions among different types of motors have been discussed for the mechanism of motor proteins during cell division (Goldstein, 1993, for a review). This idea could be supported by the presence of additional C-terminal motor, kinesin-like proteins in the same species. Recently we identified and cloned a partial sequence coding for a second C-terminal motor protein which turned out to be a CHO homologue of KIFC3 in mouse (Yang et al., 1997; Nakagawa et al., 1997) and human (Hoang et al., 1998) (R. Essner and R. Kuriyama, unpublished).

The dominant role of the minus-end-directed motor proteins in organization of the bipolar spindle is particularly prominent for *ncd* in fly oocytes where no microtubule-organizing centers are detected (Barton and Goldstein, 1996; Merdes and Cleveland, 1997, for reviews). In fact, it has long been noted that *ncd* is mutant for meiosis, but is nearly wild type for the mitotic function. Since overinduced CHO2 appears to act on the mitotic spindles in a similar manner to *ncd* in meiotic cells, this mammalian motor may primarily function during meiosis. Since the formation and establishment of spindle poles appears to be predominantly controlled by centrosomes in mitotic cells, contribution of CHO2 to the mitotic mechanism would be less prominent than in meiotic cells.

While serving as a spindle component, CHO2 may acquire

additional functions. In this regard, it would be interesting to note recent observations of CHO1/MKLP1 present in the midzonal region of the mammalian spindle (Sellitto and Kuriyama, 1988; Nislow et al., 1992). In addition to functioning in dividing cells, this plus-end-directed motor protein has been suggested to directly participate in the mechanism of microtubule organization and process formation in post-mitotic neural cells (Yu et al., 1997; Sharp 1997a). The ability of CHO2 to promote the formation of axon-like processes in transfected Sf9 cells (Sharp et al., 1997b) may indicate the possible role of this protein in neuronal tissue as well. It has recently been shown that CHO2 is in male germ cells at different developmental stages to associated with distinct microtubule-containing structures, including manchettes and sperm flagella (A. Sperry, personal communication).

We thank Ms Takako Koujin for her technical assistance for live cell fluorescence imaging. This work was supported by grants to R. Kuriyama from NIH, CTR and Minnesota Medical Foundation, to Y. Hamaguchi from Japanese Ministry, Education and Culture, P. W. Baas from NIH, and to Y. Hiraoka from the Japanese Ministry of Posts and Telecommunications.

## REFERENCES

- Barton, N. R. and Goldstein, L. S. B.** (1996). Going mobile: microtubule motors and chromosome segregation. *Proc. Nat. Acad. Sci. USA* **93**, 1735-1742.
- Bascom-Slack, C. A. and Dawson, D. C.** (1997). The yeast motor protein, Kar3p, is essential for meiosis I. *J. Cell Biol.* **139**, 459-467.
- Chandra, R., Salmon, E. D., Erickson, H. P., Lockhart, A. and Endow, S. A.** (1993). Structural and functional domains of the *Drosophila* ncd microtubule motor protein. *J. Biol. Chem.* **268**, 9005-9013.
- Davis, D. G.** (1969). Chromosome behavior under the influence of claret-nondisjunctional in *Drosophila melanogaster*. *Genetics* **61**, 577-594.
- Endow, S. A., Henikoff, S. and Soler-Niedziela, L.** (1990). Mediation of meiotic and early mitotic chromosome segregation in *Drosophila* by a protein related to kinesin. *Nature* **345**, 81-83.
- Endow, S. A., Kang, S. J., Satterwhite, L. L., Rose, M. D., Skeen, V. P. and Salmon, E. D.** (1994). Yeast Kar3 is a minus end microtubule motor protein that destabilizes microtubules preferentially at the minus end. *EMBO J.* **13**, 2708-2713.
- Endow, S. A. and Waligora, K. W.** (1998). Determinations of kinesin motor polarity. *Science* **281**, 1200-1202.
- Goldstein, L. S. B.** (1993). Functional redundancy in mitotic force generation. *J. Cell Biol.* **120**, 1-3.
- Haraguchi, T., Kaneda, T. and Hiraoka, Y.** (1997). Dynamics of chromosomes and microtubules visualized by multiple-wavelength fluorescence imaging in living mammalian cells: effects of mitotic inhibitors on cell cycle progression. *Genes Cells* **2**, 369-380.
- Hiraoka, Y. and Haraguchi, T.** (1996). Fluorescence imaging of mammalian living cells. *Chrom. Res.* **4**, 173-176.
- Hirokawa, N.** (1998). Kinesin and dynein superfamily proteins and the mechanism of organelle transport. *Science* **279**, 519-526.
- Hoang, E. H., Whitehead, J. L., Dose, A. C. and Burnside, B.** (1998). Cloning of a novel C-terminal kinesin (KIFC3) that maps to human chromosome 16q13-q21 and thus is a candidate gene for Bardet-Biedl syndrome. *Genomics* **52**, 219-222.
- Karabay, A. and Walker, R. A.** (1999). Identification of microtubule binding sites in the Ncd tail domain. *Biochemistry* **38**, 1838-1849.
- Keating, T. J., Peloquin, J. G., Rodionov, V. I., Momcilovic, D. and Borisy, G. G.** (1997). Microtubule release from the centrosome. *Proc. Nat. Acad. Sci. USA* **94**, 5078-5083.
- Kimble, M. and Church, K.** (1983). Meiosis and early cleavage in *Drosophila melanogaster* eggs: effects of the claret-non-disjunctional mutation. *J. Cell Sci.* **62**, 301-318.
- Kofron, M., Nadezhdina, E., Vassilev, A., Matulienė, J., Essner, R., Kato, J. and Kuriyama, R.** (1998). Interaction of an overinduced  $\gamma$ -tubulin with microtubules in vivo and in vitro. *Zool. Sci.* **15**, 485-495.
- Kuriyama, R., Kofron, M., Essner, R., Kato, T., Dragas-Granoic, S., Omoto, C. K. and Khodjakov, A.** (1995). Characterization of a minus-end-directed kinesin-like motor protein from cultured mammalian cells. *J. Cell Biol.* **129**, 1049-1059.
- Matthies, H. J. G., McDonald, H. B., Goldstein, L. S. B. and Theurkauf, W. E.** (1996). Anastral meiotic spindle morphogenesis: role of the non-claret disjunctional kinesin-like protein. *J. Cell Biol.* **134**, 455-464.
- McDonald, H. B. and Goldstein, L. S. B.** (1990). Identification and characterization of a gene encoding a kinesin-like protein in *Drosophila*. *Cell* **61**, 991-1000.
- McDonald, H. B., Stewart, R. J. and Goldstein, L. S. B.** (1990). The kinesin-like ncd protein of *Drosophila* is a minus end-directed microtubule motor. *Cell* **63**, 1159-1165.
- Meluh, P. B. and Rose, M. D.** (1990). KAR3, a kinesin-related gene required for yeast nuclear fusion. *Cell* **60**, 1029-1041.
- Merdes, A. and Cleveland, D. W.** (1997). Pathways of spindle pole formation: Different mechanisms; conserved components. *J. Cell Biol.* **138**, 953-956.
- Moore, J. D., Song, H. and Endow, S. A.** (1996). A point mutation in the microtubule binding region of the Ncd motor protein reduces motor velocity. *EMBO J.* **15**, 3306-3314.
- Nakagawa, T., Tanaka, Y., Matsuoka, E., Kondo, A., Okada, Y., Noda, Y., Kanai, Y. and Hirokawa, N.** (1997). Identification and classification of 16 new kinesin superfamily (KIF) proteins in mouse genome. *Proc. Nat. Acad. Sci. USA* **94**, 9654-9659.
- Nakata, T. and Hirokawa, N.** (1995). Point mutation of adenosine triphosphate-binding motif generated rogor kinesin that selectively blocks anterograde lysosome membrane transport. *J. Cell Biol.* **131**, 1039-1053.
- Nislow, C., Lombillo, V. A., Kuriyama, R. and McIntosh, J. R.** (1992). A plus-end-directed motor enzyme that moves antiparallel microtubules in vitro localizes to the interzone of mitotic spindles. *Nature* **359**, 543-547.
- Ohta, T., Kimble, M., Essner, R., Kofron, M. and Kuriyama, R.** (1995). Cell cycle-dependent expression of the CHO2 antigen, a minus-end directed kinesin-like motor in mammalian cells. *Protoplasma* **190**, 131-140.
- Pidoux, A. L., LeDizet, M. and Cande, W. Z.** (1996). Fission yeast pkl1 is a kinesin-related protein involved in mitotic spindle function. *Mol. Biol. Cell* **7**, 1639-1655.
- Sablin, E. P., Case, R. B., Dai, S. C., Hart, C. L., Ruby, A., Vale, R. D. and Fletterick, R. J.** (1998). Direction determination in the minus-end-directed kinesin motor ncd. *Nature* **395**, 813-816.
- Saunders, W., Hornack, D., Lengyel, V. and Deng, C.** (1997). The *Saccharomyces cerevisiae* kinesin-related motor Kar3p acts at preanaphase spindle poles to limit the number and length of cytoplasmic microtubules. *J. Cell Biol.* **137**, 417-431.
- Sellitto, C. and Kuriyama, R.** (1988). Distribution of a matrix component of the midbody during the cell cycle in Chinese hamster ovary cells. *J. Cell Biol.* **106**, 431-439.
- Sellitto, C., Kimble, M. and Kuriyama, R.** (1992). Heterogeneity of microtubule organizing center components as revealed by monoclonal antibodies to mammalian centrosomes and to nucleus associated bodies from *Dictyostelium*. *Cell Motil. Cytoskel.* **22**, 7-24.
- Sharp, D. J., Yu, W., Ferhat, L., Kuriyama, R., Rueger, D. C. and Baas, P. W.** (1997a). Identification of a microtubule-associated motor protein essential for dendritic differentiation. *J. Cell Biol.* **138**, 833-843.
- Sharp, D. J., Kuriyama, R., Essner, R. and Baas, P. W.** (1997b). Expression of a minus-end-directed motor protein induces Sf9 cells to form axon-like processes with uniform microtubule polarity orientation. *J. Cell Sci.* **45**, 123-131.
- Walczak, C. E., Verma, S. and Mitchison, T. J.** (1997). XCTK2: a kinesin-related protein that promotes mitotic spindle assembly in *Xenopus laevis* egg extracts. *J. Cell Biol.* **136**, 859-870.
- Walker, R. A., Salmon, E. D. and Endow, S. A.** (1990). The *Drosophila claret* segregation protein is a minus-end directed motor molecule. *Nature* **347**, 780-782.
- Yang, J. T., Laymon, R. A. and Goldstein, L. S. B.** (1989). A three-domain structure of kinesin heavy chain revealed by DNA sequence and microtubule binding analyses. *Cell* **56**, 879-889.
- Yang, Z., Hanlon, D. W., Marszalek, J. R. and Goldstein, L. S. B.** (1997). Identification, partial characterization, and genetic mapping of kinesin-like protein genes in mouse. *Genomics* **45**, 123-131.
- Yu, W., Kuriyama, R., Mallik, P. and Baas, P. W.** (1997). Inhibition of a mitotic motor protein compromises the formation of dendrite-like processes from neuroblastoma cells. *J. Cell Biol.* **36**, 659-668.